Available online at www.sciencedirect.com

ScienceDirect

Catalysis Today 119 (2007) 327–331

CATALYSIS TODAY

www.elsevier.com/locate/cattod

Mn-containing catalytic materials for the total combustion of toluene: The role of Mn localisation in the structure of LDH precursor

R. Dula *, R. Janik, T. Machej, J. Stoch, R. Grabowski, E.M. Serwicka

Institute of Catalysis and Surface Chemistry, Polish Academy of Sciences, ul. Niezapominajek 8, 30-239 Cracow, Poland

Abstract

Mg/Mn/Al mixed oxide systems of similar atomic ratios close to 2/0.5/1 were obtained by calcination of Mg,Al layered double hydroxide (LDH) type precursors containing Mn either in the cationic form within the brucite layer or as permanganate anions in the interlayer. The materials were characterised with PXRD, thermal analysis, XPS, ESR, TPR and BET. In mixed oxides derived from interlayer-doped precursor PXRD identified MgO–MnO solid solution and poorly crystalline Al-rich spinel phase, while those obtained from layer-doped LDH contained a better crystalline Mn-rich spinel. Surface of both materials was covered with poorly crystalline and/or amorphous Mn^{4+}-containing phases. Higher reducibility of this surface coat in calcined layer-doped catalyst, as compared to interlayer-doped one, was attributed to the differences in the nature of underlying crystalline phases, and was considered the chief reason for the higher catalytic activity of this catalyst in the total oxidation of toluene.

Keywords: Layered double hydroxides; Hydrotalcite; Manganese; Mixed oxides; VOCs

1. Introduction

Volatile organic compounds (VOCs) emitted during many industrial processes and transport activities contribute significantly to the atmospheric pollution [1,2] and are dangerous for the human health [3]. One of the most effective and economically attractive methods of their neutralisation is the catalytic combustion to carbon dioxide and water [4]. Oxides of the transition metals, such as Cr, Co, Cu, Ni and Mn are known as materials active in the catalytic combustion of VOCs [5–10]. The use of layered double hydroxide (LDH)-type precursors has been recognised as a very promising method of obtaining mixed oxide systems with unique structural and chemical properties [11,12]. Investigation of Mn-containing mixed oxides derived from LDH precursors concentrated on layer-doped materials [13–27], while only few studies addressed the use of LDHs containing manganese species in the interlayer [28–33].

The aim of this work was to investigate the influence of layer-doping versus interlayer-doping with manganese on the physicochemical properties and catalytic activity in the total combustion of toluene of mixed oxides obtained by calcination of starting LDHs.

2. Experimental

The layer-doped nitrate LDH denoted $MgMnAlNO_3$ was prepared by a standard co-precipitation procedure from the solution of Mg(II), Mn(II) and Al(III) nitrates, at pH 10, controlled by addition of 1 M NaOH at 50 °C. The interlayer-doped $MgAlMnO_4$ sample was prepared from the nitrate form of MgAl LDH by anion exchange with the water solution of $KMnO_4$ at a constant pH 10 at 50 °C. All syntheses were carried out in the constant flow of nitrogen. In both materials the intended ratio of Mg:Mn:Al was 2:0.5:1. Prior to catalytic tests the starting materials were converted to mixed oxide phases by 4 h calcination in air at 600 °C. The calcined samples are referred to $MgMnAlNO_3(600)$ and $MgAlMnO_4(600)$.

Samples were characterised with PXRD (Siemens D5005 diffractometer, Ni-filtered Cu Kα radiation), XPS (ESCA 150 Vacuum Science Workshop spectrometers, Al $K\alpha_{1,2}$ radiation, calibration against C 1s from adventitious carbon deposit), ESR (SE/X X-band spectrometer, Technical University, Wrocław), BET (Nova 2000 Quantachrome sorptiometer), chemical (ICP-AES Plasma 40 Perkin-Elmer spectrometer, after dissolution in

---

* Corresponding author. Tel.: +48 12 6395112; fax: +48 12 4251923.
E-mail address: ncdula@cyf-kr.edu.pl (R. Dula).

0920-5861/$ – see front matter © 2006 Elsevier B.V. All rights reserved.
doi:10.1016/j.cattod.2006.08.060

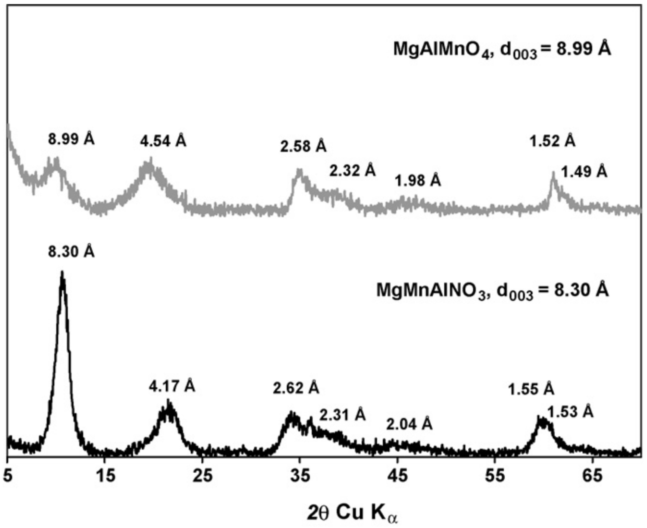

Fig. 1. XRD diagrams of the as-synthesised $MgMnAlNO_3$ and $MgAlMnO_4$ LDH samples.

nitric acid) and thermal (Derivatograph Q, static air, 25–1000 °C, heating rate 10°/min) analyses. Thermal decomposition of LDH precursors was also studied with Siemens D5005 diffractometer equipped with the high-temperature XRK unit Anthon Parr. Temperature-programmed reduction (TPR) measurements were carried out using a CHEMBET 3000 Quantachrome apparatus. Samples were heated up to 650 °C at the constant rate of 10 °C/min in the stream of the 5 vol.% H_2/Ar gas mixture at the flow rate of 30 ml/min. Catalytic tests of the total combustion of toluene were carried under atmospheric pressure in the fixed-bed flow glass reactor, in the temperature range 150–410 °C, using 0.5 ml of the catalyst, at 1.5 g/m^3 concentration of toluene in air and GHSV = 30,000 h^{-1}.

3. Results and discussion

PXRD diagrams of the starting materials, shown in Fig. 1, confirm that the solids possess LDH structure [11], with *d*(0 0 3) and *d*(0 0 6) values of 8.30 Å and 4.17 Å, respectively, observed for $MgMnAlNO_3$, and 8.99 Å and 4.54 Å, respectively, for $MgAlMnO_4$. The ratios of Mg:Mn:Al = 1.79:0.47:1.00 for $MgMnAlNO_3$ and Mg:Mn:Al = 1.73:0.44:1.00 for $MgAlMnO_4$ have been obtained from chemical analysis.

Results of XRD analysis of LDH samples calcined at 600 °C are presented in Fig. 2a. XRD pattern recorded for $MgMnAlNO_3$(600) shows that in this material crystallisation of a spinel phase of structure close to that reported for $MgMn_{1.75}Al_{0.25}O_4$ (ICSD 029221) occurred. Further thermal

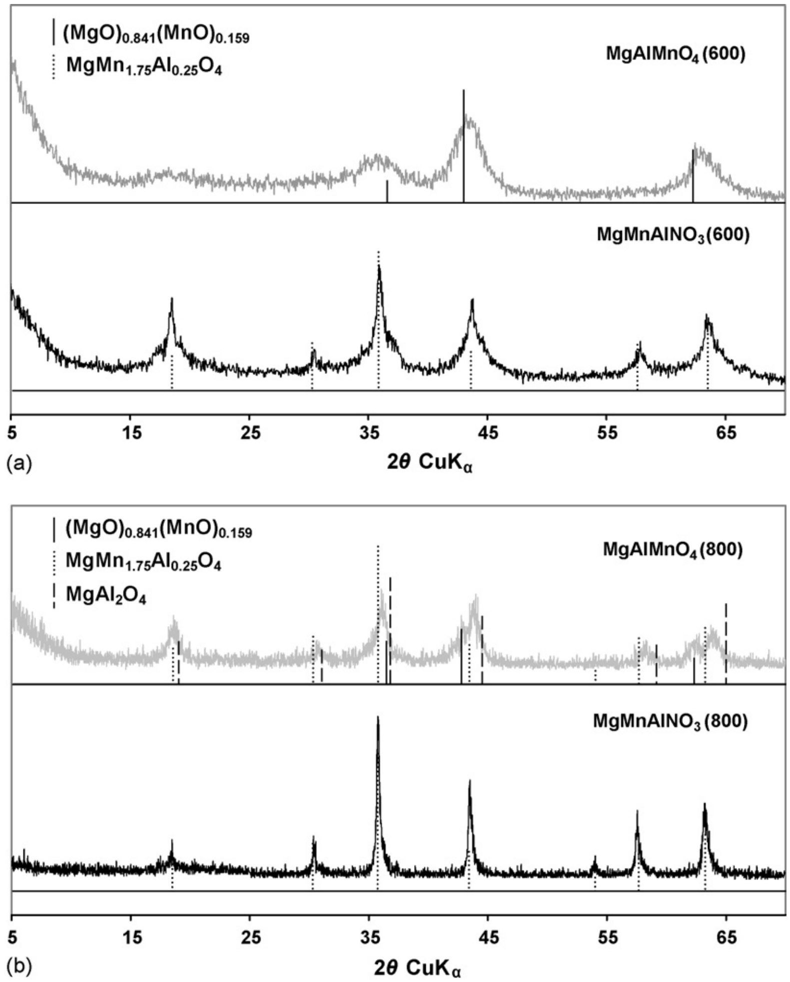

Fig. 2. XRD diagrams of $MgMnAlNO_3$ and $MgAlMnO_4$ calcined for 3 h at: (a) 600 °C and (b) 800 °C.

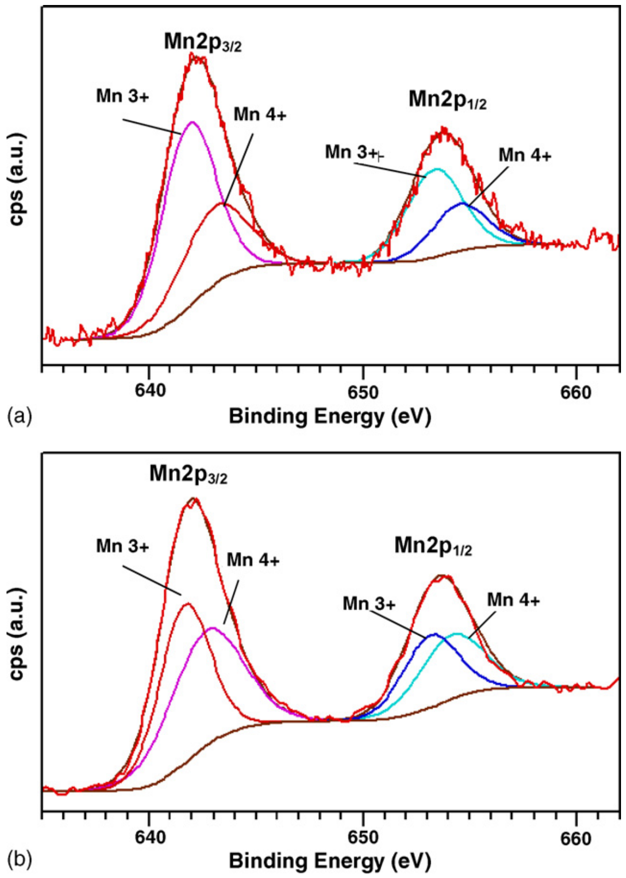

Fig. 3. XPS spectra of Mn 2p region of: (a) $MgMnAlNO_3(600)$ and (b) $MgAlMnO_4(600)$ samples.

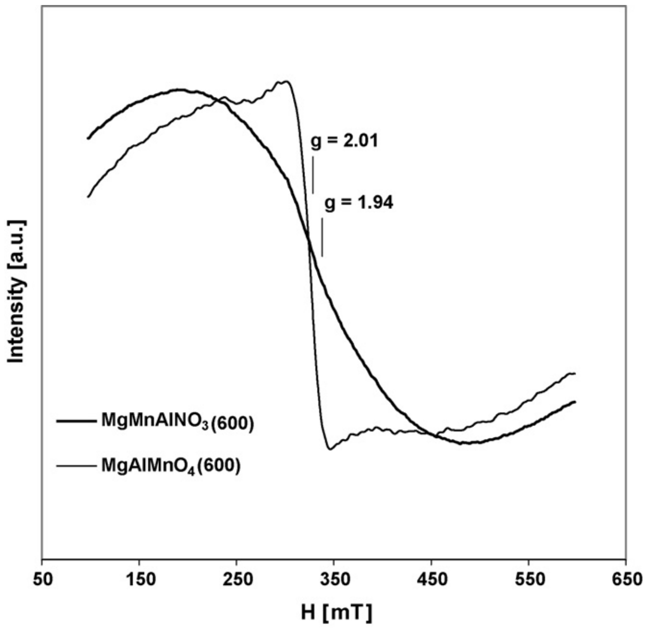

Fig. 4. ESR spectra of $MgMnAlNO_3(600)$ and $MgAlMnO_4(600)$ samples recorded at room temperature.

treatment at 800 °C improves the spinel crystallinity, but no new phases emerge (Fig. 2b). In the case of $MgAlMnO_4(600)$ broad reflections assignable to poorly crystalline MgO–MnO (ICSD 060705) solid solution are observed overlapping with an ill-defined spinel phase (Fig. 2a). The latter becomes more crystalline in the material subjected to thermal treatment at 800 °C (Fig. 2b). Comparison with the reference pattern of $MgMn_{1.75}Al_{0.25}O_4$ shows that here the reflections, especially at higher 2θ are shifted towards slightly higher values, than in the case of spinel present in the $MgMnAlNO_3(800)$, and closer to the positions reported for $MgAl_2O_4$ (ICSD 029444). This indicates that the chemical composition of spinel structure evolving in calcined $MgAlMnO_4$ differs from that formed in calcined $MgMnAlNO_3$ by containing less Mn^{3+} and more Al^{3+}. The specific surface area of mixed oxide materials prepared for the catalytic tests by calcination of the precursors at 600 °C is 137 and 191 m^2/g for $MgMnAlNO_3(600)$ and $MgAlMnO_4$ ‘(600), respectively, in agreement with the XRD data pointing to the better crystallinity of the former (Fig. 2a). The XPS analysis of calcined samples shows that in the $Mn2p_{3/2}$ region the spectrum may be decomposed into two components (Fig. 3; Table 1). On the basis of the literature data the observed binding energies may be tentatively associated with the presence of Mn^{4+} and Mn^{3+} ions [34–37]. It has to be born in mind that identification of the oxidation state of surface manganese species on the basis of $2p_{3/2}$ binding energies is associated with a high degree of uncertainty due to the overlap of energy ranges reported for various oxidation states of Mn. The Mn 3s exchange splitting, considered a more accurate means to determine the nature of manganese ions [34,38–40], could not be applied in the present case due to the strong overlap with Mg 2s peaks. For this reason we have analysed the difference between the binding energies of $Mn2p_{3/2}$ and O1s levels, shown to depend on the oxidation state of the relevant Mn species [35,41]. The observed values, presented in Table 1, correspond closely to those reported for Mn^{3+} and Mn^{4+}, which support the assignment derived from the analysis of the $Mn2p_{3/2}$ binding energies. Since the crystalline phases identified by means of XRD contain Mn at +2 and/or +3 oxidation states, this result indicates that Mn^{4+} containing phases, which exist at the

Table 1
$Mn2p_{3/2}$ and O1s binding energies, FWHM and relative intensities of the different manganese species in calcined samples

Sample	$Mn2p_{3/2}$ (BE) [eV]	$Mn2p_{3/2}$ (FWHM) [eV]	O1s (BE) [eV]	O1s (FWHM) [eV]	ΔE^* [eV]	Ion	Area [%]
$MgMnAlNO_3(600)$	641.83	2.97	529.68	2.16	112.15	Mn^{3+}	65.4
	643.01	3.69			113.33	Mn^{4+}	34.6
$MgAlMnO_4(600)$	641.63	2.78	529.7	2.17	111.93	Mn^{3+}	51.0
	642.62	3.98			112.92	Mn^{4+}	49.0

$^*\Delta E = BE(Mn2p_{3/2}) - BE(O1s)$.

surface of the calcined samples are of poorly crystalline and/or amorphous nature.

The existence of phases containing Mn^{4+} ions is confirmed by ESR spectroscopy, which can detect Mn^{2+} and Mn^{4+}, but not Mn^{3+}. Fig. 4 shows the ESR spectra of $MgMnAlNO_3(600)$ and $MgAlMnO_4(600)$ recorded at room temperature. Both are dominated by a broad ($\Delta B = 340$ mT) signal with $g = 1.94$, characteristic of closely interacting Mn^{4+} (as in MnO_2) [42,43]. Additionally, in the spectrum of $MgAlMnO_4(600)$, a component with $g = 2.01$ and $\Delta B = 48$ mT can be seen, pointing to the existence of Mn^{2+} centres. The lack of hyperfine splitting indicates that the Mn^{2+} ions concerned are in close proximity to each other [44,45]. The appearance of this signal corroborates the identification of MnO–MgO solid solution phase in this material.

The TPR profiles of both mixed oxide catalysts, presented in Fig. 5, show that the materials possess considerably different reducibilities. While the highest hydrogen consumption occurs in both samples around 500 °C, there is an obvious shift in the area corresponding to the lowest and the highest temperature regimes, pointing to the better reducibility of $MgMnAlNO_3(600)$. This sample contains easily reducible material responsible for hydrogen uptake at 250–400 °C, and lacks component responsible for high temperature TPR profile of $MgAlMnO_4(600)$. In view of the multiple oxidation states identified in both materials, the beginning of reduction corresponds to $Mn^{4+} \rightarrow Mn^{3+}$ transition, while the high temperature part of both TPR curves to $Mn^{3+} \rightarrow Mn^{2+}$ transitions, the complexity of the profiles being due to the multiphase composition of the investigated mixed oxides [46–53]. Thus, the results show that the surface Mn^{4+}/Mn^{3+}-containing phase (or phases) is much more reducible in $MgMnAlNO_3(600)$ than in $MgAlMnO_4(600)$, and that in the latter a Mn^{3+}-containing phase exists (or is formed), which is more difficult to reduce and is responsible for the hydrogen uptake above 550 °C. The differences in the high temperature region may be attributed to the different chemical nature of spinel phases present in both samples, the one identified in $MgAlMnO_4(600)$ and containing more Al^{3+} being more difficult to reduce. In view of the known effect of the nature of the support on the reducibility of surface manganese phases [47] it is likely that the differences in reduction rate of Mn^{4+} containing surface layers are due to the different character of the crystalline phases present in both samples. Thus, better reducibility observed for $MgMnAlNO_3(600)$ would be the result of the deposition of Mn-containing surface coat on the manganese-rich spinel, while interaction with aluminium-rich spinel and/or MnO–MgO solid solution would result in lower reducibility of the surface Mn^{4+} present in $MgAlMnO_4(600)$.

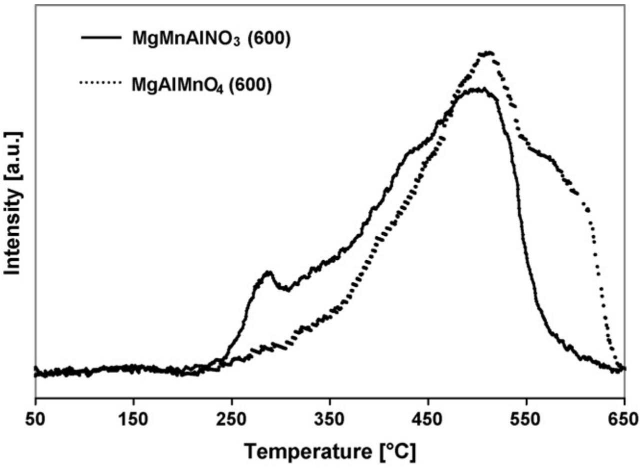

Fig. 5. TPR curves of $MgMnAlNO_3(600)$ and $MgAlMnO_4(600)$ samples.

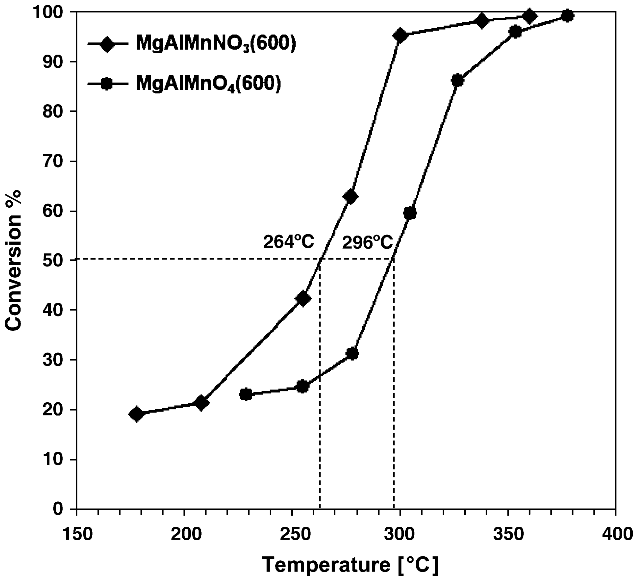

Fig. 6. Temperature dependence of the toluene conversion at GHSV 30,000 h^{-1} for $MgMnAlNO_3(600)$ and $MgAlMnO_4(600)$ catalysts.

The manner of the incorporation of manganese into the structure of LDH precursor strongly influences the catalytic activity of calcined samples in the reaction of total combustion of toluene. The temperature profiles of toluene conversion, presented in Fig. 6, show that the catalyst derived from the layer-doped precursor constitutes a more active material than that obtained from interlayer-doped LDH. Comparison of the light-off T_{50} values (the temperature of 50% conversion) of the catalysts, marked in Fig. 6, with the $T_{50} = 262$ °C obtained under similar conditions for a commercial VOC catalyst (Katalizator Ltd.) shows that the catalytic activity of the $MgMnAlNO_3(600)$ material is very attractive.

It has been repeatedly demonstrated that the activity of Mn-based catalysts for the total oxidation of VOCs is associated with their reducibility [53–55]. Indeed, the TPR experiments show that the more active $MgMnAlNO_3(600)$ material, in particular its Mn^{4+}-containing surface component, is more easily reduced than the $MgAlMnO_4(600)$ sample. Thus, it appears that the catalytic activity of the mixed oxides derived from the layer-doped precursor depends on the redox properties of Mn^{4+}/Mn^{3+} system present within the surface oxidic layer, which in turn are controlled by the nature of underlying supporting phases.

4. Conclusions

Localisation of manganese in the structure of Mg,Al LDH determines the properties of mixed oxide materials obtained by thermal decomposition of appropriate precursors. Calcination of interlayer-doped MgAlMnO$_4$ LDH leads to formation of MgO–MnO solid solution and nucleation of poorly crystalline Al-rich spinel phase, while calcination of layer-doped MgMnAlNO$_3$ LDH results in the formation of better crystalline Mn-rich spinel. Surface of both materials is covered with poorly crystalline and/or amorphous Mn^{4+}-containing phases. Higher reducibility of calcined layer-doped catalyst as compared to interlayer-doped one is associated with the differences in samples phase composition. In particular, differences in the reduction rate of Mn^{4+}-containing surface coats are attributed to the different nature of the underlying crystalline phases. Mixed oxide catalyst obtained from the layer-doped MgMnAlNO$_3$ LDH is more active in the combustion of toluene than the one obtained from the permanganate-intercalated precursor. Enhanced activity of the former is assigned to the better reducibility of the amorphous surface layer containing the Mn^{4+}/Mn^{3+} redox system.

Acknowledgement

This work was supported by the Ministry of Scientific Research and Information Technology within the research project 3 T09A 066 27.

References

[1] M.J. Molina, Pure Appl. Chem. 68 (1996) 1749.
[2] R. Atkinson, Atmos. Environ. 34 (2000) 2063.
[3] R. Lauwerys, Toxicologie Industrielle et Intoxications Professionnelles, third ed., Masson, Paris, 1992.
[4] L.D. Pfefferle, L.C. Pfefferle, Catal. Rev. Sci. Eng. 29 (1987) 219.
[5] J.J. Spivey, Ind. Eng. Chem. Res. 26 (1987) 2165.
[6] J.J. Spivey, J.B. Butt, Catal. Today 11 (1992) 465.
[7] J.J. Spivey, in: G.C. Bond, G. Webb (Senior Reporters), Complete Oxidation of Volatile Organics, Catalysis, vol. 8, The Royal Society of Chemistry, Cambridge, 1989, p. 157.
[8] R. Prasad, L.A. Kennedy, E. Ruckenstein, Catal. Rev. Sci. Eng. 26 (1984) 1.
[9] M.F.M. Zwinkels, S.G. Järas, P.G. Menon, T.A. Griffin, Catal. Rev. Sci. Eng. 35 (1993) 319.
[10] K. Bahranowski, E. Bielańska, R. Janik, T. Machej, E.M. Serwicka, Clay Miner. 34 (1999) 67.
[11] F. Cavani, F. Trifiró, A. Vaccari, Catal. Today 11 (1991) 173.
[12] A. Vaccari, Appl. Clay Sci. 14 (1999) 161.
[13] C. Barriga, J.M. Fernandez, M.A. Ulibarri, F.M. Labajos, V. Rives, J. Solid State Chem. 124 (1996) 205.
[14] S. Velu, C. Swamy, J. Mater. Sci. Lett. 15 (1996) 1674.
[15] S. Velu, C. Swamy, React. Kinet. Catal. Lett. 62 (1997) 339.
[16] S. Velu, N. Shah, T.M. Jyothi, S. Sivasanker, Microporous Mesoporous Mater. 33 (1999) 61.
[17] K. Jiratova, P. Cuba, F. Kovanda, L. Hilaire, V. Pitchon, Catal. Today 76 (2002) 43.
[18] S. Aisawa, H. Hirahara, H. Uchiyama, S. Takahashi, E. Narita, J. Solid State Chem. 167 (2002) 152.
[19] F. Kovanda, T. Grygar, V. Dornicak, Solid State Sci. 5 (2003) 1019.
[20] L. Obalova, M. Valaskova, F. Kovanda, Z. Lacny, K. Kolinova, Chem. Pap. 58 (2004) 33.
[21] T. Grygar, T. Rojka, P. Bezdicka, E. Vecernikova, F. Kovanda, J. Solid State Electrochem. 8 (2004) 252.
[22] V.R. Choudhary, D.K. Dumbre, B.S. Uphade, V.S. Narkhede, J. Mol. Catal. A Chem. 215 (2004) 129.
[23] F. Li, L. Zhang, D.G. Evans, X. Duan, Colloid Surf. A 244 (2004) 169.
[24] A. Chen, H. Xu, Y. Yue, W. Hua, W. Shen, Z. Gao, Appl. Catal. A Gen. 274 (2004) 101.
[25] A. Chen, H. Xu, Y. Yue, W. Hua, W. Shen, W. Hua, Z. Gao, Ind. Eng. Chem. Res. 43 (2004) 6409.
[26] A. Chen, H. Xu, W. Hua, W. Shen, Y. Yue, Z. Gao, Top. Catal. 35 (2005) 177.
[27] F. Kovanda, T. Grygar, V. Dornicak, T. Rojka, P. Bezdicka, K. Jiratova, Appl. Clay Sci. 28 (2005) 121.
[28] T. Sato, T. Wakabayashi, M. Shimada, Ind. Eng. Chem. Prod. Res. Dev. 25 (1986) 89.
[29] T. Yamagishi, Y. Oyanagi, E. Narita, Nippon Kagaku Kaishi 4 (1993) 329.
[30] H. Shimada, K. Saito, Nippon Kagaku Kaishi 5 (1997) 335.
[31] Y. Guo, D. Li, Ch. Hu, E. Wang, Y. Zou, H. Ding, S. Feng, Microporous Mesoporous Mater. 56 (2002) 153.
[32] J.C. Villegas, O.H. Giraldo, K. Laubernds, S.S. Suib, Inorg. Chem. 42 (2003) 5621.
[33] V.R. Choudhary, J.R. Indurkar, V.S. Narkhede, R. Jha, J. Catal. 227 (2004) 257.
[34] B. Gillot, S. Buguet, E. Kester, C. Baubet, Ph. Tailhades, Thin Solid Films 357 (1999) 223.
[35] M. Oku, K. Hirokawa, S. Ikeda, J. Electron Spectrosc. Relat. Phenom. 7 (1975) 465.
[36] V. Di Castro, G. Polzonetti, J. Electron Spectrosc. Relat. Phenom. 48 (1989) 117.
[37] J.S. Foord, R.B. Jackman, G.C. Allen, Philos. Magn. A 49 (1984) 657.
[38] C.S. Fadley, D.A. Shirley, Phys. Rev. A 2 (1970) 1109.
[39] I. Barrio, I. Legorburu, M. Montes, M.I. Dominguez, M.A. Centeno, J.A. Odriozola, Catal. Lett. 101 (2005) 151.
[40] V.R. Galakhov, M. Demeter, S. Bartkowski, M. Neumann, N.A. Ovechkina, E.Z. Kurmaev, N.I. Lobachevskaya, Ya.M. Mukovskii, J. Mitchell, D.L. Ederer, Phys. Rev. B 65 (2002) 113102.
[41] P. Decorse, G. Caboche, L.-C. Dufour, Solid State Ionics 117 (1999) 161.
[42] M. Kakazey, N. Ivanova, Y. Boldurev, S. Ivanov, G. Sokolsky, J.G. Gonzalez-Rodriguez, M. Vlasova, J. Power Sources 114 (2003) 170.
[43] R. Stoyanova, E. Zhecheva, S. Vassilev, J. Sol. State. Chem. 179 (2006) 378.
[44] K. Dyrek, Bull. Acad. Polon. Sci. Ser. Sci. Chim. 22 (1974) 213.
[45] M. Occhiuzzi, D. Cordischi, R. Dragone, Phys. Chem. Chem. Phys. 5 (2003) 4938.
[46] F. Kapteijn, L. Singoredjo, A. Andreini, Appl. Catal. B Environ. 3 (1994) 173.
[47] F. Arena, T. Torre, C. Raimondo, A. Parmaliana, Phys. Chem. Chem. Phys. 3 (2001) 1911.
[48] L. Christel, A. Pierre, A.M. Duprat, A. Rousset, Thermochim. Acta 306 (1997) 51.
[49] A. Russo Sorge, M. Turco, G. Pilone, G. Bagnasco, J. Propulsion Power 20 (2004) 1069.
[50] L. Lisi, G. Bagnasco, P. Ciambelli, S. De Rossi, P. Porta, G. Russo, M. Turco, J. Solid State Chem. 146 (1999) 176.
[51] S. Cimino, L. Lisi, S. De Rossi, M. Faticanti, P. Porta, Appl. Catal. B Environ. 43 (2003) 397.
[52] G. Fierro, M. Lo Jacono, M. Inversi, R. Dragone, G. Ferraris, Appl. Catal. B Environ. 30 (2001) 173.
[53] P. Ciambelli, S. Cimino, S. De Rossi, M. Faticanti, L. Lisi, G. Minelli, I. Pettiti, P. Porta, G. Russo, M. Turco, Appl. Catal. B Environ. 24 (2000) 243.
[54] V.A. de la Peña O'Shea, M.C. Alvarez-Galvan, J.L.G. Fierro, P.L. Arias, Appl. Catal. B Environ. 57 (2005) 191.
[55] S. Royer, H. Alamdari, D. Duprez, S. Kaliaguine, Appl. Catal. B Environ. 8 (2005) 273.